

Dynamics of Lennard-Jones clusters: A characterization of the activation-relaxation technique

Rachid Malek* and Normand Mousseau†

Department of Physics and Astronomy and CMSS, Ohio University, Athens, Ohio 45701

(Received 2 June 2000)

The potential energy surface of Lennard-Jones clusters is investigated using the activation-relaxation technique (ART). This method defines events in the configurational energy landscape as a two-step process: (a) a configuration is first activated from a local minimum to a nearby saddle-point and (b) is then relaxed to a new minimum. Although ART has been applied with success to a wide range of materials such as *a*-Si, *a*-SiO₂ and binary Lennard-Jones glasses, questions remain regarding the biases of the technique. We address some of these questions in a detailed study of ART-generated events in Lennard-Jones clusters, a system for which much is already known. In particular, we study the distribution of saddle-points, the pathways between configurations, and the reversibility of paths. We find that ART can identify all trajectories with a first-order saddle point leaving a given minimum, is fully reversible, and samples events following the Boltzmann weight at the saddle point.

PACS number(s): 82.20.Wt, 66.10.Cb, 02.70.Lq, 82.20.Kh

I. INTRODUCTION

In many materials and systems, microscopic structural relaxation takes place on time scales much longer than those of the atomistic oscillations set by the phonon vibrations (10 ps). This is the case, for example, for glasses and other complex materials. Such a time spread in the dynamics can be understood from the configurational energy landscape picture. Indeed, the system finds itself in a deep minimum surrounded by energy barriers much higher than its thermal energy and only rare fluctuations can allow the system to jump over a barrier and move to a new minimum. These long time scales are especially prohibitive for numerical studies using traditional methods such as molecular dynamics and real-space Monte Carlo, which are tied to the phonon time scale.

One way to reach this long time scale is through activated dynamics [1–3]. In this case, the algorithm focuses directly on the appropriate mechanisms and describes the dynamics as a sequence of metastable states separated by energy barriers. These metastable configurations can be well identified by their atomic positions at zero K, which correspond to a local minimum in the configurational energy landscape. Knowledge of the distribution and properties of these local minima is sufficient to determine the thermodynamical properties of the system. A proper description of the dynamics, however, also requires knowledge of the rates controlling jumps from one local minimum to another.

Activated dynamics has been successfully applied to a range of discrete problems. It has turned out to be especially useful in the study of metallic surfaces, where it is possible to identify and compute *a priori* the whole set of barriers to be visited during the dynamics [4]. These methods have also been applied, with further approximations, to other systems such as the hetero-epitaxial growth of semiconductor compounds [5]. Such simulations can reach simulated times 10

or 12 orders of magnitude longer than what can be done with molecular dynamics.

For more complex systems, however, identifying the barriers and insuring proper statistical sampling remain a challenge. The activation-relaxation technique (ART) [3,6] was proposed recently to address this challenge. A number of questions remain regarding the biases of the method, how it samples the potential energy landscape and whether or not it is reversible.

Before achieving the long-term objective of developing an algorithm for simulating the atomistic time evolution of complex materials, it is necessary to address these issues. Here, we answer some of these questions in a study of Lennard-Jones (LJ) clusters, comparing the ART of Barkema and Mousseau with a similar algorithm introduced by Doye and Wales (DW) [7]. In particular, we look at the sampling of barriers, the reversibility of the paths from the saddle point and from the new minimum. The dynamical and thermodynamical properties of LJ clusters have been thoroughly studied [8–10] and they provide an ideal model for the development of global optimization techniques [11–13] as well as activated methods.

This paper is constructed as follows. In the next section, we describe the details of the activation-relaxation technique. We then present the results of our simulation on three different LJ clusters (13, 38, and 55 atoms) and give a short discussion.

II. TECHNIQUE

The activation-relaxation technique, [3,6] is a generic method to explore the surface energy landscape and search for saddle points. It has been applied with success to amorphous semiconductors, silica, and metallic glasses [3,6,14–17].

ART defines events in the configurational energy landscape according to a two-step process: (a) starting from a local minimum, a configuration is pushed up to a local saddle point, representing the activation process; (b) from this saddle point, the configuration is relaxed into a new minimum; this whole process is called an event. For the activa-

*Email address: malek@helios.phy.ohiou.edu

†Email address: mousseau@helios.phy.ohiou.edu

tion, we use a modified version of the algorithm, ART *nouveau*, which was introduced recently [18]. In this version, we follow the eigenvector corresponding to the largest, negative eigenvalue of the Hessian, ensuring a full convergence onto the saddle point. This is similar in spirit to the hybrid conjugate-gradient/conjugate-gradient method introduced recently by Munro and Wales [19].

The configuration is first pushed along a random direction until a negative eigenvalue appears. At each step along this trajectory, its total energy is relaxed in the hyperplane perpendicular to it. This ensures that the total energy and forces remain under control as the configuration leaves the harmonic well.

Once the lowest eigenvalue passes a threshold (set here at 10^{-3}), we start the convergence to the saddle point by pushing the configuration along the eigenvector corresponding to this lowest eigenvalue, while minimizing the forces in all other directions. Unless the lowest eigenvalue turns positive, this procedure is guaranteed to converge onto a first-order saddle point, where forces on the configuration are zero. If the lowest eigenvalue changes sign, the iteration procedure is stopped and a new event is started.

Because ART is designed to work for systems with thousands of degrees of freedom, it is not appropriate to perform a direct diagonalization of the Hessian to extract eigenvalues and eigenvectors. We use instead the Lanczos algorithm [20,21]. This algorithm works by iteratively projecting a vector on the Hamiltonian, extracting preferably the lowest eigenvalues and corresponding eigenvectors. In our case, 15–30 force evaluations are sufficient to extract the very lowest eigenvalue and its eigenvector, requiring the diagonalization of a tridiagonal matrix of the same dimensions. As a bonus, this iterative scheme can use the direction of the previous step as a seed, ensuring a better convergence.

The second step of the algorithm, the relaxation, is straightforward and can be achieved with any standard minimization technique. We use the conjugate gradient (CG) method [22].

Since moves are defined directly in the $3N$ -dimensional configurational space, ART is not sensitive to the constraints of real space algorithms: a complex collective motion, requiring the displacement of hundreds of atoms, is as easily produced as a one-atom jump; and a high energy barrier does not require more efforts to cross than a thermal one. Such versatility is particularly important in disordered and complex materials where events can involve collective rearrangements that are hard to foresee.

In this work, the energy landscape is described by the Lennard-Jones potential:

$$E = 4\epsilon \sum_{i < j} \left[\left(\frac{\sigma}{r_{ij}} \right)^{12} - \left(\frac{\sigma}{r_{ij}} \right)^6 \right], \quad (1)$$

where ϵ is the pair well depth and $2^{1/6}\sigma$ is the equilibrium pair separation. The energy and distance are described below in units of ϵ and σ , respectively.

As mentioned above, we compare our results to those obtained by the Doye and Wales (DW) version of ART. DW propose a systematic technique for exploring the surface energy landscape. Transition states are found by using the eigenvector-following method [23–25], in which the energy

is maximized along one direction and simultaneously minimized in all the others. In this approach, the Hessian matrix is diagonalized at the local minimum and each of its eigenvectors are followed in turn in both directions away from this minimum. Although there is no information regarding the position of saddle points in the Hessian at the local minimum, the eigenvalue of the eigenvectors followed from this point often moves down and, at some point, might become negative. From then on, the procedure is similar to that described above.

The main advantage of this algorithm is that it provides a systematic way of exploring the local energy landscape, moreover, we can expect that its biases will be different from those of ART *nouveau* described above. It suffers some limitations, however. First, the number of trial directions is finite, leading to a maximum of $6N$ saddle points. As we will see below, even in small clusters, this is not enough to sample all saddle points. Second, the method requires the full diagonalization of the Hessian matrix repeatedly, at least in its first stage, making it an order N^3 technique, too costly for problems of more than a few hundred degrees of freedom. This later limitation was recently removed by Munro and Wales with the introduction of a hybrid eigenvector-following scheme [19].

III. SIMULATIONS

Simulations are done for the 13-atom, 38-atom, and 55-atom Lennard-Jones clusters, using both ART and DW. In all cases, we start from a relatively well-relaxed generic configuration, i.e., one which does not have special symmetries, and explore the energy landscape around this minimum. The goal here is not to recreate the full connectivity tree—but this was done already by Doye *et al.* [26]—but to study the biases of the methods in finding events.

A. A comparison between ART and DW

For DW, the number of search directions is limited to $6N$. A number of these directions do not converge to a saddle point or lead to degenerate activated points, producing of order N structurally different saddles. Contrary to DW, ART can generate an infinite number of initial search directions. In the first part of the simulation, we limit ourselves to sets of 3000 trial events, starting from the same initial minimum, for each cluster size.

After eliminating degenerate saddle configurations, ART is found to have generated three to four times more events than DW for these clusters. This ratio is, of course, related to the number of trial directions used in the ART simulation. As discussed below, for example, a 20 000 trial run on the 13-atom cluster can find all first-order paths leaving a given local minimum.

Results for these runs, including statistics on the saddle points and new configurations are reported in Table I. In all cases, permutational isomers are eliminated and only structurally different configurations are counted.

The sets of saddle points and minima obtained by ART and DW are obviously not independent and we find, as one would expect, a significant overlap between them: about 80% of DW events are also found by the 3000-attempt run of

TABLE I. Number of structurally different saddle points and new minima (i.e., after eliminating configurational isomers) as a function of the number of trial directions for the 13-atom, the 38-atom, and the 55-atom LJ clusters. For DW, all 6N possible directions are tried. For ART, results presented here are based on 3000-event runs. Ranges of activation and asymmetry energies (minimum and maximum) are given in units of ϵ .

Methods		DW	ART	Common
13-atoms	Saddles	17	72	13
	New minima	13	44	13
	Activation	0.54-3.62	0.54-3.68	
	Asymmetry	(-0.05)-2.75	(-0.05)-3.57	
38-atoms	Saddles	28	109	23
	New minima	21	73	21
	Activation	0.26-3.2	0.14-5.66	
	Asymmetry	(-0.88)-2.64	(-1.64)-3.1	
55-atoms	Saddles	42	151	35
	New minima	29	89	29
	Activation	0.65-5.98	0.65-9.34	
	Asymmetry	(-1.84)-3.98	(-1.84)-8.22	

ART (while about 20% of ART events are also found by DW).

We can do a similar analysis for the new minima found by the two methods. Table I shows that in many cases, a number of different saddle points lead to the same final minimum. Moreover, this degeneracy seems to increase with the size of the cluster. (The existence of multiple paths connecting two minima is much more common for open systems, such as clusters, than for bulk materials. In the later case, the constraints of volume and continuity make it much more difficult to find many paths connecting two events.) For all cluster sizes, the 3000-trial event ART simulations finds about three times more minima than the DW method, a ratio similar to the saddle configurations.

B. Ergodicity and reversibility

It is possible to examine the question of the ergodicity of ART by extending the simulations described above. In Fig. 1, we trace the number of different saddle points and minima

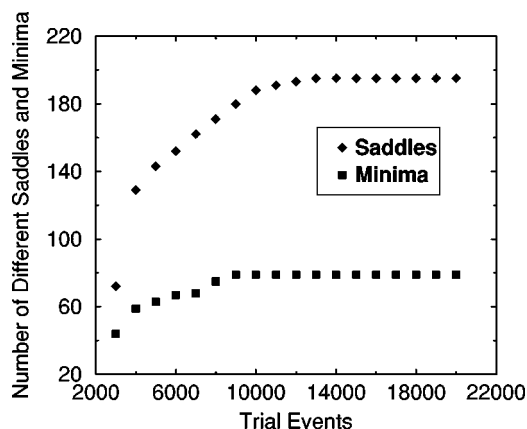


FIG. 1. Number of different saddle points and minima as a function of the number of trial events for a 20 000-attempt ART run the 13-atoms LJ cluster.

as a function of trial events in a 20 000-attempt run, using a single initial minimum as in the previous simulation. The sampling of minima seems to be complete after about 9000 events and we identify a total of 79 different minima, including all those found using the DW method. It takes about 50% more events to generate all 195 saddle points that can be found with ART. Here again, all saddle points generated with DW are found by ART. Although this does not show formally the completeness of the sets found, the previous simulation, as well as its comparison with a different technique, provides a fairly solid base for claiming that ART is ergodic.

Dynamically, events should also be fully reversible. We check this in a two-step simulation. First, we check the reversibility of the paths from the saddle point. After converging to a first-order saddle point, we pull the configuration back very slightly and apply the relaxation routine from there. For the 3000 ART-generated events on the 13-atom LJ cluster, all but 10 (0.33%) events relax to the original minimum and these last 10 events converge to a different but very close local minimum. Saddle points found by ART are therefore really delineating the boundary of the energy basin around the initial minimum.

Clearly, paths are fully reversible from their activated point.

The full trajectory must also be reversible; the initial minimum, saddle, final minimum sequence should also be found in the opposite order. For each LJ cluster, we select 20 new local minima, reached in a one-step event from the initial minimum and check that, indeed, the configuration can always come back to that state, and that the same saddle points are found in both directions. This important result allows us to conclude that the whole pathway between local minima passing through first-order saddle points is reversible.

C. Stability under change of parameters

In the search for saddle points, a number of factors can influence the selection of the activation paths. In particular, it is important to verify that the step size along the direction of the lowest eigenvalue, in the convergence to the saddle point, does not result in some events missing. To examine this issue, we perform the same simulation as that described above for the 13-atom LJ cluster with two different step values: 0.01σ and 0.03σ . The distribution of energy barriers for all converged saddle points is given in Fig. 2. All saddle points found by the 0.01σ step are also found by the larger step. Moreover, the 0.03σ seems to better converge to higher energy barriers. The total number of saddle points reached by using 0.03σ step value is also four times greater than that found by 0.01σ . This sheds some light on the workings of the algorithm. As we follow the eigendirection corresponding to the lowest eigenvalue, the configuration is in a very narrow and shallow valley in a high-dimensional space and too much relaxation perpendicular to this valley can easily bring it in a region of non-negative curvature. With a larger step moving away from the minimum, the configuration reaches a deep valley faster, increasing strongly the rate of convergence. It is clear, here, that this parameter can be adjusted to optimize the rate of convergence without fear of losing particular saddle points.

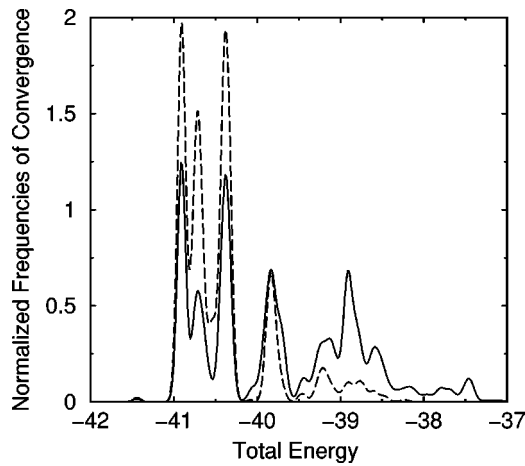


FIG. 2. Normalized frequencies of occurrence in the case of 13-atom LJ clusters for two-step values 0.01σ and 0.03σ . The solid curve corresponds to the case of 0.03σ and the dashed one to 0.01σ . The total energy is given in units of ϵ .

D. Biases in searching for saddle points

We now address the question of biases in the search for saddle points and new minima. The range of activation and asymmetry energies is quite wide for the events generated on the three clusters, as can be seen in Table I. As expected, this range increases with the size of the system. This behavior is typical of clusters. For bulk systems, the distribution of relevant activation events is generally independent of the size and is usually bounded by a small multiple of the binding energy between two atoms. The higher bound for the distribution of activation energy reflects the overall properties of the systems studied and should be independent of the starting configuration; the lower bound, however, is not; it represents a direct measure of the stability of the initial metastable state.

Figure 3 gives two representations of the distribution of activation and asymmetry energies for the 55-atom clusters. In Fig. 3(a), we give the distribution of energies for the 151 different saddles and 89 different minima identified in the 3000-trial event run. The distribution of saddle energies is rather smooth over its whole range while that of the asymmetry energies presents a few peaks.

To study the biases of ART, we also plot in Fig. 3(b) and (c) the normalized distribution of activation and asymmetry energies for *all* 1856 completed ART events and the corresponding 109 successful DW events (although there are a total of 330 trial directions for DW, the method shows a poor success rate when eigendirections corresponding to very high eigenvalues are selected.) The distribution for DW is therefore almost discretized and peaks correspond to single saddle points being visited many times. The ART distribution is almost continuous and we have binned the events as a function of energy.

The structure of these distributions is quite different from that of Fig. 3(a). In particular, they are strongly peaked at low energies indicating that each method seems to enhance significantly a few paths over the other ones. The biases are not exactly the same, however, although there is considerable overlap for the two methods. This suggests that the topography of the energy landscape around the minimum is reflected, at least in part, in the choice of events: the algo-

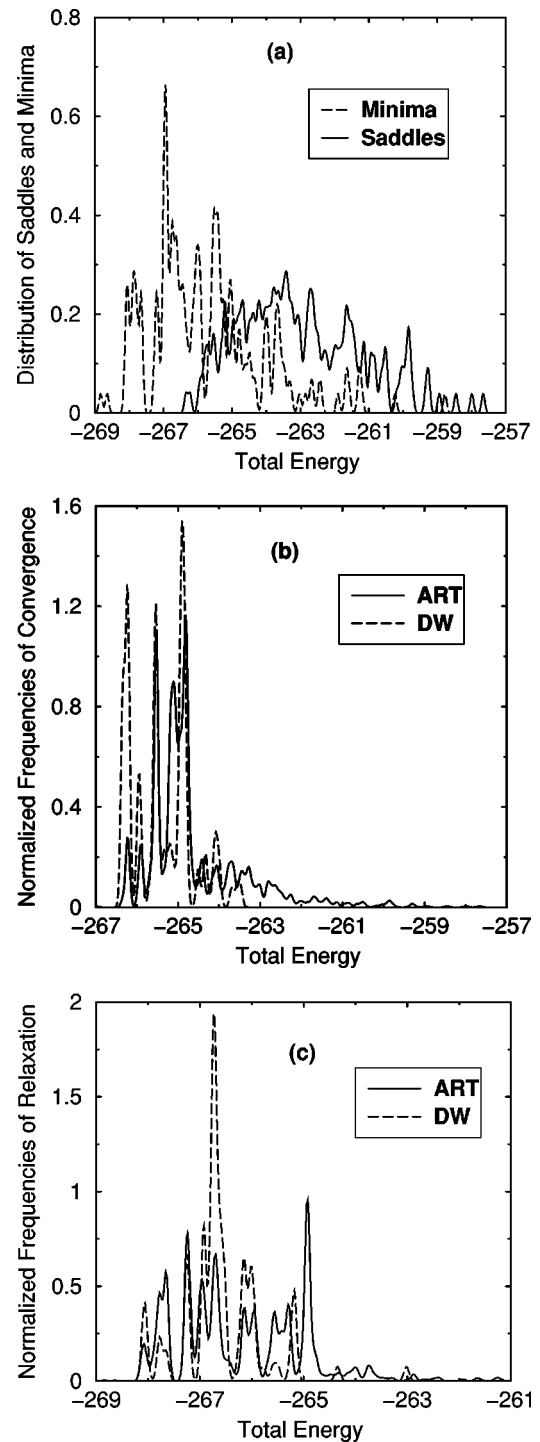


FIG. 3. (a) The distribution of saddle points and minima as a function of energy for the 55-atom clusters as found in a 3000-trial event ART run leading to 1856 completed events. (b) Normalized frequency of occurrence of saddle points as a function of energy for the ART and DW runs for the same cluster. The DW run generated 109 successful events. (c) Same as (b), but for minima. In both (b) and (c), the solid curve represents ART and the dashed one DW. The total energy is given in units of ϵ .

rihm retained for leaving the harmonic well clearly influences the biases of the method.

One approach to identify the overall biases of ART is to plot the ratio of the distribution of barriers for all saddle points generated (frequency of convergence) over that of the

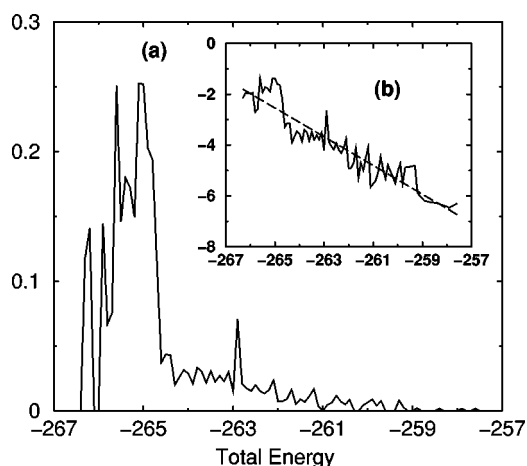


FIG. 4. (a) Ratio of the distribution of barriers for all saddle points generated in a 3000-attempt ART run [Fig. 3(a)] over that of the different saddle points existing around a minimum [Fig. 3(b)]. The same distribution is plotted in inset (b) with a log-normal scale. The dashed line is a fit with slope -0.57 . The total energy is given in unit of ϵ .

different saddle points existing around our minimum. This ratio, plotted in Fig. 4, provides a first indication on how ART selects saddle points. In Fig. 4(a), the distribution is dominated by a strong peak at low activation energy, followed by a fairly extended tail. Surprisingly, most of the small structure that can be found in 3(a) has been eliminated in the ratio, indicating that there is fairly little bias toward a few events in particular but that the selection of an event over another one is mostly a matter of energy. This can be seen more clearly in the log-normal distribution plotted in Fig. 4(b). The result is remarkable: the distribution is well fitted by an exponential function $p(E) \propto \exp(-0.57E)$ and the sampling follows a Boltzmann distribution. The same behavior can be observed for the 13-atom and the 38-atom clusters, as shown in Fig. 5.

IV. CONCLUSION

The configurational energy landscape of Lennard-Jones clusters was explored by using the activation-relaxation technique (ART). Comparing ART with a different sampling method proposed by Doye and Wales, it does not seem that ART missed any class of first-order activated paths. Based on this and extensive simulations, we conclude that ART can

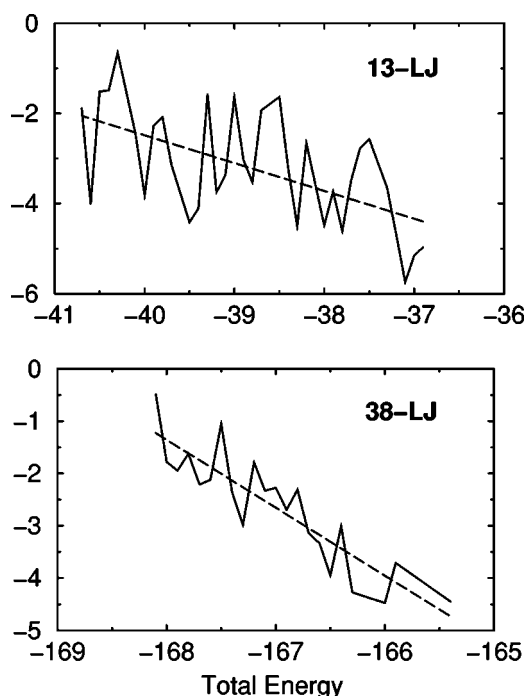


FIG. 5. Same as previous figure for the 13-atom and the 38-atom LJ clusters. The slope of the fitted line is -0.62 and -1.3 , respectively. The total energy is given in units of ϵ .

find all first-order saddle points and new minima around a given minimum, indicating that it is ergodic. The trajectories it defines, initial minimum–saddle point–final minimum, are also reversible, indicating that the trajectories found are real activated paths.

We find, finally, that ART samples the surface energy landscape according to a Boltzmann distribution, i.e., that the probability of finding a given saddle point is proportional to $\exp(E_{\text{barrier}}/E_0)$. The origin of this bias is not yet understood but this opens the door to real-time activated dynamics in complex systems.

ACKNOWLEDGMENTS

We acknowledge useful discussions with G. Barkema as well as partial financial support from the NSF under Grant No. DMR-9805848.

[1] A.F. Voter, Phys. Rev. Lett. **78**, 3908 (1997).
 [2] G.T. Barkema, M.J. Howard, and J.L. Cardy, Phys. Rev. E **53**, 2017 (1996).
 [3] G.T. Barkema and N. Mousseau, Phys. Rev. Lett. **77**, 4358 (1996).
 [4] See, for example, M. Breeman, G. Rosenfeld, and G. Comsa, Phys. Rev. B **54**, 16 640 (1996); J.G. Amar and F. Family, Surf. Sci. **382**, 170 (1997); F.M. Bulnes, V.D. Pereyra, and J.L. Ricardo, Phys. Rev. E **58**, 86 (1998); A.F. Voter *et al.* J. Chem. Phys. **80**, 5814 (1984); M. Breeman *et al.*, Thin Solid Films **272**, 195 (1996).
 [5] See, for example, J. Wang and A. Rockett, Phys. Rev. B **43**, 12

571 (1991); C. Roland and G.H. Gilmer, Phys. Rev. Lett. **67**, 3188 (1991); S. Wilson, *Chemistry by Computer* (Plenum, New York, 1986); M. Djafari-Rouhani *et al.*, Mater. Sci. Eng., B **44**, 82 (1997); M. Djafari-Rouhani, R. Malek, I. Kersulis, and V. Mitin, Microelectron. J. **28**, 1043 (1997); M. Djafari-Rouhani, R. Malek, and D. Esteve, Thin Solid Films **318**, 61 (1998).
 [6] N. Mousseau and G.T. Barkema, Phys. Rev. E **57**, 2419 (1998).
 [7] J.P.K. Doye and D.J. Wales, Z. Phys. D: At., Mol. Clusters **40**, 194 (1997).
 [8] J. Pillardy and L. Piela, J. Phys. Chem. **99**, 11805 (1995).

- [9] R.H. Leary, *J. Global Optim.* **11**, 35 (1997).
- [10] D.J. Wales and J.P.K. Doye, *J. Phys. Chem. A* **101**, 5111 (1997).
- [11] M.R. Hoare and J. McInnes, *Faraday Discuss. Chem. Soc.* **61**, 12 (1976).
- [12] C.J. Tsai and K.D. Jordan, *J. Phys. Chem.* **97**, 11227 (1993).
- [13] F.H. Stillinger, *Phys. Rev. E* **59**, 48 (1999).
- [14] G.T. Barkema and N. Mousseau, *Phys. Rev. Lett.* **81**, 1865 (1998).
- [15] N. Mousseau, G.T. Barkema, and S.W. de Leeuw, *J. Chem. Phys.* **112**, 960 (2000).
- [16] N. Mousseau and L.J. Lewis, *Phys. Rev. Lett.* **56**, 9461 (1997).
- [17] N. Mousseau and G.T. Barkema, *IEEE Comput. Sci. Eng.* **1**, 74 (1999).
- [18] N. Mousseau, e-print cond-mat/0004356.
- [19] L.J. Munro and D.J. Wales, *Phys. Rev. B* **59**, 3969 (1999).
- [20] C. Lanczos, *Applied Analysis* (Dover, New York, 1988).
- [21] Otto F. Sankey, David A. Drabold, and Andrew Gibson, *Phys. Rev. B* **50**, 1376 (1994).
- [22] W.H. Press *et al.*, *Numerical Recipes* (Cambridge University Press, Cambridge, 1988).
- [23] J. Pancir, *Collect. Czech. Chem. Commun.* **40**, 1112 (1974).
- [24] C.J. Cerjan and W.H. Miller, *J. Chem. Phys.* **75**, 2800 (1981).
- [25] D.J. Wales, *J. Chem. Phys.* **101**, 3750 (1994).
- [26] J.P.K. Doye, M.A. Miller, and D.J. Wales, *J. Chem. Phys.* **111**, 8417 (1999).